CORE
Metadata, citation and similar papers at core.ac.uk
Provided by CERN Document Server

PHYSICAL REVIEW D **73,** 015010 (2006)

Treatment of threshold effects in supersymmetric spectrum computations

H. Baer,[1] J. Ferrandis,[2] S. Kraml,[3] and W. Porod[4,5]
[1]*Dept. of Physics, Florida State University, Tallahassee, Florida 32306, USA*
[2]*Lawrence Berkeley Laboratory, Berkeley, California 94720, USA*
[3]*Theory Division, Dept. of Physics, CERN, CH-1211 Geneva 23, Switzerl*
[4]*Instituto de Física Corpuscular, CSIC, València, Spain*
[5]*Institut für Theoretische Physik, Univ. Zürich, Switzerland*
(Received 8 December 2005; published 20 January 2006)

We take a critical view of the treatment of threshold effects in SUSY spectrum computations from high-scale input. We discuss the two principal methods of (a) renormalization at a common SUSY scale versus (b) integrating out sparticles at their own mass scales. We point out problems in the implementations in public spectrum codes, together with suggestions for improvements. In concrete examples, we compare results of Isajet 7.72 and SPheno 2.2.3, and present the improvements done in Isajet 7.73. We also comment on theoretical uncertainties. Last but not least, we outline how a consistent multiscale approach may be achieved.

DOI: 10.1103/PhysRevD.73.015010 PACS numbers: 12.60.Jv

I. INTRODUCTION

It is often argued [1–4] that, from measurements of supersymmetry (SUSY) at the LHC and ILC, the model parameters can be extracted precisely enough to test the high-scale structure of the theory, in other words to test the boundary conditions of the soft SUSY-breaking (SSB) terms. This requires relating, with very high precision, sparticle properties measured at the TeV energy scale with the Lagrange parameters at the high-energy scale, often the GUT-scale.

Of course, the question arises as to what theoretical uncertainties are involved in this exercise. Such uncertainties originate from truncating the perturbation series of (a) the running of the $\overline{\rm DR}$ parameters between the electroweak (EW) and the high-energy scale, and (b) the relation at the EW scale between $\overline{\rm DR}$ and on-shell SUSY parameters. They have been investigated in [5] by comparing different state-of-the-art spectrum computations. Differences at the level of a few per cent have been found, part of which have been traced to higher-order loop effects. Since then important improvements have been made in all codes. When comparing today the latest versions of Isajet [6], SoftSusy [7], SPheno [8] and Suspect [9], the typical spread in the results is $-0.9 \lesssim 1\%$, which is compatible with the expected precisions at the LHC and getting close to those expected at the planned International Linear Collider (ILC) (see [10] for an online comparison).

One exception is the mass of the lightest neutralino. On the one hand, $m_{\tilde{\chi}_1^0}$ is expected to be measured with permille precision at the ILC. On the other hand, in mSUGRA with a binolike LSP, one finds differences of few per cent in the $m_{\tilde{\chi}_1^0}$ obtained from Isajet 7.72 as compared to $m_{\tilde{\chi}_1^0}$ obtained from SoftSusy 2.0, SPheno 2.2.3 or Suspect 2.3.4 (these latter three programs typically agree to $\sim$0.5% on $m_{\tilde{\chi}_1^0}$). In this context it should also be noted that a $\sim$1 GeV error in the mass of the LSP can translate into a $\sim$10% error in the prediction of its relic density [11].

The public spectrum codes under consideration all have 2-loop renormalization group (RG) running implemented. A major difference between Isajet on the one side and SoftSusy, SPheno and Suspect on the other lies in the treatment of threshold effects for computing the sparticle pole masses. This is the topic of this paper. It was the above mentioned discrepancy in the prediction of the LSP mass that motivated this study. Our analysis, however, applies to the computation of the pole masses of mixing sparticles in general.

The paper is organized as follows. In Sec. II we briefly explain the two methods used to compute the sparticle pole masses. In Sec. III we review these methods for the example of the neutralino sector. We compare results of SPheno 2.2.3 and Isajet 7.72, and discuss some shortcomings in the computations as well as ways of improving. In Sec. IV we then analyze the scalar top sector. An improved scheme for the computation of sparticle masses in Isajet is presented in Sec. V. The technical difficulties involved with a consistent multiscale approach are discussed in more detail in Sec. VI, and finally Sec. VII contains our conclusions.

II. TWO METHODS

The RG equations are employed in the $\overline{\rm DR}$ scheme. The SUSY mass parameters obtained from the RG evolution are hence $\overline{\rm DR}$ running ones. In order to obtain the physical sparticle masses one therefore has to perform the proper shifts to the on-shell scheme. The public SUSY spectrum codes can in fact be classified by their method of determining the sparticle pole masses.

 © 2006 The American Physical Society

One approach, adopted by SoftSusy, SPheno and Suspect[1], is to assume that the full set of MSSM RGEs (gauge and Yukawa couplings plus soft terms) are valid between the scales M_Z and $M_{\rm GUT}$. The gauge and Yukawa coupling boundary conditions are stipulated at $Q = M_Z$, while soft term boundary conditions are stipulated at $Q = M_{\rm GUT}$. The RGEs are run iteratively between M_Z and $M_{\rm GUT}$ until a convergent solution is found. The $\overline{\rm DR}$ parameters are extracted at a common renormalization scale Q, usually taken to be $Q = M_{\rm SUSY} = \sqrt{m_{\tilde{t}_L} m_{\tilde{t}_R}}$ or $\sqrt{m_{\tilde{t}_1} m_{\tilde{t}_2}}$. The one-loop (logarithmic and finite) self-energy corrections [12] are then added at that scale [2]. We will refer to this method as ''common scale approach''. It is relatively straightforward and certainly self-consistent, but misses two-loop logarithmic contributions between the renormalization scale Q and the actual mass scale of the sparticle. Such logarithmic corrections could be relevant in cases where the mass scales involved are severely split, such as in focus-point supersymmetry.

The other method, proposed in [14,15], is to adopt a multiscale effective theory approach, and to functionally integrate out all heavy degrees of freedom at each particle threshold. As this is realized by the use of a theta function at each threshold, we call it the ''step-beta function approach'' (implying continuous matching conditions for the remaining parameters). The program Isajet does adopt a hybrid technique along these lines. In Isajet 7.72, the full two-loop MSSM RGEs are employed between M_Z and $M_{\rm GUT}$, with the exception that one-loop step-beta functions are adopted for gauge and Yukawa couplings. (This approach means that log corrections to gauge and Yukawa couplings at the scale $Q = M_Z$ are not needed, since they are handled by the RG evolution). In addition, each SSB parameter m_i is extracted from the RGEs at an energy scale equal to $m_i = m_i(m_i)$, with the exception of parameters involved in the Higgs potential, which are all extracted at the common scale $Q = M_{\rm SUSY} = \sqrt{m_{\tilde{t}_L} m_{\tilde{t}_R}}$.

The RG evolution of mass parameters from high to low scales is equivalent to computing the logarithmic radiative corrections. The step-beta function approach hence gives a leading-log approximation of $m_i = m_i(m_i)$. For sparticles that do not mix, i.e. gluinos as well as squarks and sleptons of the first and second generations, this approach directly gives the pole masses up to constant terms. For the required level of precision these constant terms are important, so they have to be added at the end of the running. The situation is more complicated for mixing sparticles, since multiple mass scales can be involved in the mixing matrices, and care has to be taken to compute the on-shell mass matrices in a consistent way. This will be discussed in more detail in the following sections, first for the example of the neutralino sector, and then for the case of scalar tops. Moreover, as we will discuss in Sec. VI, at the two-loop level, each time a sparticle is integrated out this implies nontrivial matching conditions for the parameters remaining in the effective theory. To our knowledge these matching conditions are not yet known and, thus, are not yet taken into account properly. There are also other complications, which we will discuss in Sec. VI.

III. NEUTRALINO SECTOR

A. Neutralino mass matrix

At lowest order, the neutralino mass matrix in the basis $\psi_j^0 = (-i\lambda', -i\lambda^3, \psi_{H_1}^0, \psi_{H_2}^0)$ is

$$\mathcal{M}_N = \begin{pmatrix} M_1 & 0 & -m_Z s_W c_\beta & m_Z s_W s_\beta \\ 0 & M_2 & m_Z c_W c_\beta & -m_Z c_W s_\beta \\ -m_Z s_W c_\beta & m_Z c_W c_\beta & 0 & -\mu \\ m_Z s_W s_\beta & -m_Z c_W s_\beta & -\mu & 0 \end{pmatrix} \tag{1}$$

with $s_W = \sin\theta_W$, $c_W = \cos\theta_W$, $s_\beta = \sin\beta$, $c_\beta = \cos\beta$ and $\tan\beta = v_2/v_1$. It is diagonalized by a unitary mixing matrix N:

$$N\mathcal{M}_N N^T = \mathrm{diag}(\varepsilon_1 m_{\tilde{\chi}_1^0}, \varepsilon_2 m_{\tilde{\chi}_2^0}, \varepsilon_3 m_{\tilde{\chi}_3^0}, \varepsilon_4 m_{\tilde{\chi}_4^0}), \tag{2}$$

where $m_{\tilde{\chi}_i^0}$ $(i = 1, \ldots, 4)$ are the neutralino masses, $m_{\tilde{\chi}_1^0} < \ldots < m_{\tilde{\chi}_4^0}$, and ε_i are their signs. The mass eigenstates are $\tilde{\chi}_i^0 = N_{ij}\psi_j^0$.

The SUSY parameters taken out of the RG running are $\overline{\rm DR}$ parameters at a certain scale Q. Straightforward diagonalization of Eq. (1) therefore gives the $\overline{\rm DR}$ running mass eigenvalues. In order to obtain the neutralino pole masses, one has to add self-energy corrections

$$\mathcal{M}_N^{\rm onshell} = \mathcal{M}_N(Q) + \Delta\mathcal{M}_N(Q), \tag{3}$$

leading to corrections in the masses, $m_{\tilde{\chi}_i^0} \to m_{\tilde{\chi}_i^0} + \Delta m_{\tilde{\chi}_i^0}$, and in the mixing matrix $N \to N + \Delta N$. Here notice that the on-shell condition $p^2 = m^2$ has to be fulfilled for each $m_{\tilde{\chi}_i^0}$ separately; so one has to diagonalize Eq. (3) 4 times[3]. The corrections at the one-loop level are given in [12]; see also the discussion in [16]. They typically amount to a few per cent. Since the shift from the $\overline{\rm DR}$ to the on-shell sheme, Eq. (3), cannot be performed to all orders, there will always

[1]Early versions of Suspect used the step-beta function approach described below; the method of a common renormalization scale is used from version 2.0 onwards.

[2]For the neutral Higgs masses and the μ parameter, also the two-loop corrections of [13] are included.

[3]This actually leads to a (numerically very small) ambiguity in the neutralino mixing matrix. In Isajet 7.69-7.72, tree-level mixing elements are adopted for cross section calculations, along with loop-corrected neutralino masses. In SPheno 2.2.3, the mixing matrix obtained for $p^2 = m^2_{\tilde{\chi}_1^0}$ is used.

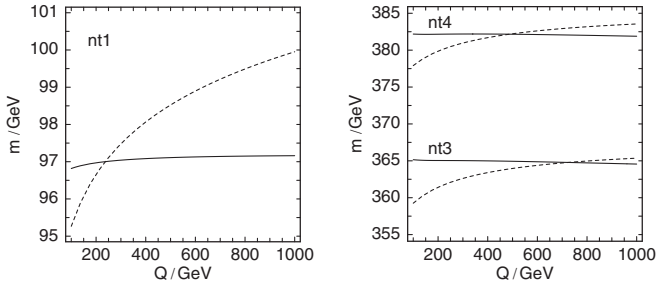

FIG. 1. Dependence of the masses of $\tilde{\chi}_1^0$ (left) and $\tilde{\chi}_{3,4}^0$ (right) on the renormalization scale Q. The dashed lines are the $\overline{\rm DR}$ running masses, the full lines are the one-loop-corrected pole masses. Computed with SPheno 2.2.3.

be a small residual scale dependence of the pole masses. This scale dependence is often regarded as an estimate of higher-order corrections.

In the step-beta function approach, the mass parameters that enter Eq. (1) are $M_1(M_1)$, $M_2(M_2)$, and $\mu(M_{\rm SUSY})$. According to [15], this corresponds to the on-shell $\mathcal{M}_N$ up to finite corrections. The on-shell mass matrix at the full one-loop level is then given by

$$\mathcal{M}_N^{\rm onshell} = \mathcal{M}_N^{\rm log.corr} + \Delta\mathcal{M}_N^{\rm const}. \tag{4}$$

The complications involved in this procedure will be discussed in Sec. VI.

B. Threshold corrections at a common scale

We first discuss results for the approach of running all SUSY-breaking parameters to a common renormalization scale Q and adding one-loop threshold corrections at this scale. As already mentioned, this is the method employed in SoftSusy, SPheno and Suspect. We use the mSUGRA benchmark point SPS1a with

$$\begin{aligned} m_0 = 100, \qquad m_{1/2} = 250, \qquad A_0 = -100, \\ \tan\beta = 10, \qquad \mu > 0, \qquad m_t = 175 \end{aligned} \tag{5}$$

as an illustrative numerical example. Moreover, we take $\alpha_s(M_Z) = 0.1172$, and $m_b(m_b) = 4.214$ GeV as SM input values in the $\overline{\rm MS}$ scheme so as to be able to compare with Isajet 7.72.

The dependence of the $\overline{\rm DR}$ running (tree-level) neutralino masses and the one-loop-corrected pole masses on the scale Q is shown in Fig. 1, for $Q = 100$ GeV to 1 TeV. In addition, Table I lists the $\overline{\rm DR}$ mass parameters together with the tree-level and one-loop-corrected neutralino masses at SPS1a for some particular choices of Q. The numbers have been obtained with SPheno 2.2.3, which has the complete one-loop corrections of [12] for all sparticle masses. As can be seen, going from the $\overline{\rm DR}$ to the on-shell scheme is a quite important correction. The scale dependence of the $\overline{\rm DR}$ (or tree-level) neutralino masses, $m_{\tilde{\chi}_i^0}^{\overline{\rm DR}}$, is about 5 GeV between $Q = 100$ GeV and $Q = 1$ TeV. That is about 5% for the LSP mass and about 2–3% for the masses of the heavier neutralinos. For the one-loop-corrected pole masses, $m_{\tilde{\chi}_i^0}^{\rm pole}$, the scale dependence goes down to the level of a few permille. Here notice also that the scale dependence is largest for the winolike $\tilde{\chi}_2^0$.

The results of SoftSusy 2.0 and Suspect 2.3.4 are very similar to those of SPheno 2.2.3. For illustration the results obtained with Suspect 2.3.4 are listed in Table II. Here the scale dependence of $m_{\tilde{\chi}_{2,3}^0}^{\rm pole}$ is slightly larger, because the self-energy corrections are applied in the approximation given in Sect. 4.2 in [12].

The scale dependence gives an estimate of the size of the missing higher-order logarithmic corrections. This is not necessarily the full theoretical uncertainty. One point of caution is, for instance, the fact the SUSY threshold cor-

TABLE I. Parameters and masses (in GeV) for the mSUGRA benchmark point SPS1a obtained with SPheno 2.2.3 for different renormalization scales Q; $M_{\rm SUSY} = 484.5$ GeV.

Q	M_1	M_2	μ	$m_{\tilde{\chi}_1^0}^{\overline{\rm DR}}$	$m_{\tilde{\chi}_2^0}^{\overline{\rm DR}}$	$m_{\tilde{\chi}_3^0}^{\overline{\rm DR}}$	$m_{\tilde{\chi}_4^0}^{\overline{\rm DR}}$	$m_{\tilde{\chi}_1^0}^{\rm pole}$	$m_{\tilde{\chi}_2^0}^{\rm pole}$	$m_{\tilde{\chi}_3^0}^{\rm pole}$	$m_{\tilde{\chi}_4^0}^{\rm pole}$
100	98.39	188.9	352.7	95.27	173.3	359.3	377.9	96.82	179.9	365.2	382.2
200	99.78	190.1	355.0	96.66	174.8	361.4	379.9	96.97	180.3	365.0	382.2
$M_{\rm SUSY}$	101.6	191.7	357.6	98.47	176.6	363.9	382.2	97.11	180.7	364.9	382.2
1000	103.1	193.0	359.2	99.95	178.0	365.4	383.5	97.16	181.0	364.6	381.9

TABLE II. Same as Table I, but computed with Suspect 2.3.4; $M_{\rm SUSY} = 465.4$ GeV.

Q	M_1	M_2	μ	$m_{\tilde{\chi}_1^0}^{\overline{\rm DR}}$	$m_{\tilde{\chi}_2^0}^{\overline{\rm DR}}$	$m_{\tilde{\chi}_3^0}^{\overline{\rm DR}}$	$m_{\tilde{\chi}_4^0}^{\overline{\rm DR}}$	$m_{\tilde{\chi}_1^0}^{\rm pole}$	$m_{\tilde{\chi}_2^0}^{\rm pole}$	$m_{\tilde{\chi}_3^0}^{\rm pole}$	$m_{\tilde{\chi}_4^0}^{\rm pole}$
100	98.55	188.9	352.6	95.25	173.3	358.5	377.2	97.00	179.7	363.4	382.4
200	99.96	190.2	354.8	96.66	174.7	360.5	379.1	97.18	180.2	363.0	381.9
$M_{\rm SUSY}$	101.5	191.6	356.7	98.38	176.4	363.0	381.3	97.31	180.8	362.8	381.7
1000	103.3	193.1	358.9	99.96	177.9	364.4	382.7	97.37	181.2	362.1	381.0

TABLE III. Isajet results (in GeV) for the neutralino sector at SPS1a. Case A is the original Isajet 7.72; Case B is Isajet 7.72 with the improvement that the one-loop self-energies are each computed at their relevant scale as explained in the text; and Case C employs step-beta functions for all SUSY parameters. In case D, the SUSY parameters are all frozen out at $M_{\rm SUSY} = 456$ GeV, and the one-loop corrections are applied at this scale.

Case	M_1	M_2	μ	$m^{(0)}_{\tilde{\chi}^0_1}$	$m^{(0)}_{\tilde{\chi}^0_2}$	$m^{(0)}_{\tilde{\chi}^0_3}$	$m^{(0)}_{\tilde{\chi}^0_4}$	$m^{(1)}_{\tilde{\chi}^0_1}$	$m^{(1)}_{\tilde{\chi}^0_2}$	$m^{(1)}_{\tilde{\chi}^0_3}$	$m^{(1)}_{\tilde{\chi}^0_4}$
A	99.5	192.4	351.2	96.2	176.4	358.0	377.0	95.2	180.5	357.0	377.5
B	99.5	192.4	351.2	96.2	176.4	358.0	377.0	97.9	182.0	357.6	377.9
C	103.2	192.9	345.1	99.9	176.4	351.5	371.4	101.5	181.7	351.6	372.6
D	101.7	192.1	350.9	98.4	176.2	357.9	376.9	97.3	180.2	356.7	377.2

rections to the gauge and Yukawa couplings are computed collectively at M_Z. This is a valid choice. However, the matching between SM and MSSM couplings could also be done at, for instance, $m_{\rm LSP}$ or $M_{\rm SUSY}$. The thus induced uncertainty is not taken into account by the scale dependence as it results in a shift in the boundary conditions.

C. Step-beta functions in Isajet

In the implementation employed in Isajet 7.72, each SSB parameter (aside from Higgs potential parameters) is extracted from the RG running at the scale equal to the SSB mass value. In particular, the parameters in the neutralino sector are $M_1(M_1)$, $M_2(M_2)$, $\mu(M_{\rm SUSY})$ and $\tan\beta(M_{\rm SUSY})$ [4]. In this way logarithmic threshold corrections are included, and diagonalizing the tree-level mass matrix of Eq. (1) gives a leading-log approximation of the neutralino pole masses. Finite corrections, however, can be of the same order as the logarithmic ones, so they have to be taken into account according to Eq. (4).

At this point some comments are in order on the actual implementation of the step-beta function approach in Isajet. Up to and including Isajet version 7.72:

(i) While the SSB parameters are extracted from the RG running at their respective mass scale, the SSB parameters are not formally ''integrated out'', so that the soft term RGEs remain those of the MSSM all the way from $M_{\rm GUT}$ to M_Z (unlike the case of the gauge and Yukawa couplings, where the beta functions change each time a threshold is passed). Thus, the Isajet algorithm is actually a mixed scheme.

(ii) For the finite shifts, the full expressions of [12] for the one-loop self-energies are used. These involve A_0, B_0 and B_1 functions, which depend on the renormalization scale Q and are evaluated at $Q = M_{\rm SUSY}$ in Isajet 7.69-7.72. This leads to a double counting of logs between $M_{\rm SUSY}$ and the actual mass scale of the sparticle.

[4]Inside Isajet, $M_{\rm SUSY}$ is called HIGFRZ and given by HIGFRZ=SQRT(MAX(AMZ**2,AMTLSS*AMTRSS*SIGN(1.,AMTLSS*AMTRSS))).

Numerically Isajet 7.72 agrees quite well with the other public codes. The exception is the LSP mass, which, as already mentioned in the introduction, typically turns out to be a few per cent smaller than the results from SoftSusy 2.0, Suspect 2.3.4 and SPheno 2.2.3. This can be understood as an effect of the above mentioned double counting, which induces an error $\propto \ln(\tilde{m}^2/M^2_{\rm SUSY})$, where $\tilde{m}$ is the mass parameter of the sparticle considered. Obviously, the effect is largest for the LSP.

As a concrete example, the results of Isajet 7.72 for the parameters of SPS1a, Eq. (5), are given as Case A in Table III. Here $m^{(0)}_{\tilde{\chi}^0_i}$ corresponds to the 'leading-log' approximation while $m^{(1)}_{\tilde{\chi}^0_i}$ is the final result including the ''finite'' corrections. We note a difference of about 6 GeV in $\mu(M_{\rm SUSY})$ with respect to SPheno 2.2.3, which is however not of immediate concern for this analysis (it mainly stems from the different loop order of the effective Higgs potential in the two programs). More important for us is the 2 GeV difference in the LSP pole mass due to the choice of scale for the self-energy corrections.

As a first step of improvement, we modify Isajet 7.72 so that the one-loop self-energies for each neutralino (and also for each other sparticle) are computed with the renormalization scale set to its own mass scale. This means always setting the variable XLAM in the routine SSM1LP to the mass of the sparticle being renormalized. In this way, the double counting is much reduced. The result is shown as Case B in Table III. As expected, while the effect on the heavy neutralino masses is small, there is a shift upwards of 2 GeV in the LSP mass.

Next we invoke the complete step-beta functions of Ref. [15] into the RGEs of *all* the SUSY parameters. The result of this is shown as Case C in Table III. As can be seen, the agreement with the other codes is less good in this case. One reason is that when integrating out one parameter, this leads in principle also to finite shifts for the parameters that remain in the RGEs. This is, however, not taken into account in the ''naive'' step-beta function approach, which employs continuous matching conditions. We will discuss this and other issues in more detail in Sec. VI.

As a consistency check, we also freeze out all SUSY parameters at $Q = M_{\rm SUSY}$ in Isajet, and compute the pole masses at this scale analogous to what is done in the other codes. This is shown as Case D in Table III and indeed gives the expected level of agreement with the other codes.

IV. SCALAR TOP SECTOR

We next discuss the scalar top (stop) sector. At the tree level, the stop mass matrix is given by

$$\mathcal{M}_{\tilde{t}}^2 = \begin{pmatrix} m_{\tilde{t}_L}^2 & a_t h_t \\ a_t h_t & m_{\tilde{t}_R}^2 \end{pmatrix} = \begin{pmatrix} M_{\tilde{Q}_3}^2 + m_t^2 + D_L & (A_t v_2 - \mu v_1) h_t \\ (A_t v_2 - \mu v_1) h_t & M_{\tilde{U}_3}^2 + m_t^2 + D_R \end{pmatrix}, \quad (6)$$

where $D_{L,R}$ denote the D-term contributions, $v_{1,2}$ are the Higgs VEVs and h_t is the top Yukawa coupling. Using $h_t = m_t/v_2$, the off-diagonal element can also be written as

$$a_t h_t = (A_t - \mu \cot\beta) m_t, \quad (7)$$

with m_t the running top-quark mass. The difference to the neutralino sector is that this off-diagonal element can be large, actually as large or even larger than the diagonal elements. It can hence introduce a large mixing of $\tilde{t}_L$ and $\tilde{t}_R$, and much enhance the splitting of the mass eigenstates $\tilde{t}_{1,2}$.

This is not a problem in the common scale approach, where all the parameters are taken at the same scale and therefore

$$(\mathcal{M}_{\tilde{t}}^2)^{\rm onshell} = \mathcal{M}_{\tilde{t}}^2(Q) + \Delta\mathcal{M}_{\tilde{t}}^2(Q), \quad (8)$$

with $\Delta\mathcal{M}_{\tilde{t}}^2(Q)$ the one-loop self-energy corrections given in [12]. Again, they have to be computed once for $\tilde{t}_1$ and once for $\tilde{t}_2$. This also results in a small $\mathcal{O}(1\%)$ difference in the stop mixing angle, depending on whether it is taken at $p^2 = m_{\tilde{t}_1}^2$ or $p^2 = m_{\tilde{t}_2}^2$.

In the step-beta function approach applied in Isajet 7.72, the lowest-order mass matrix given in terms of $M_{\tilde{Q}_3}^2(M_{\tilde{Q}_3}^2)$, $M_{\tilde{U}_3}^2(M_{\tilde{U}_3}^2)$, $A_t(A_t)$, $\mu(M_{\rm SUSY})$, $v_{1,2}(M_{\rm SUSY})$ and $h_t(M_{\rm SUSY})$, and it becomes quite involved to define the corrections to the on-shell scheme in a consistent way. It is hence more convenient to integrate out all stop parameters at the average scale $Q_{\tilde{t}} = M_{\rm SUSY} = \sqrt{m_{\tilde{t}_L} m_{\tilde{t}_R}}$ and add the self-energy corrections as in Eq. (8).

Table IV shows the results of SPheno 2.2.3 for the stop sector at SPS1a for different renormalization scales Q. As can be seen, the scale dependence of the pole masses at one loop is about 1.5%, that is $\mathcal{O}(\alpha_s^2)$.

Table V shows the results of Isajet for Cases A–D, analogous to Sec. III C. Case B has a somewhat higher $\tilde{t}_1$ mass than Cases A,D and SPheno 2.2.3. This can be explained by the fact that the $\tilde{t}_1$ and $\tilde{t}_2$ masses are not, respectively, evaluated at $p^2 = m_{\tilde{t}_1}^2$ and $p^2 = m_{\tilde{t}_2}^2$ in Isajet 7.72, but both at $p^2 = m_{\tilde{t}_L}^2$. Case C has somewhat lower top squark masses. The reason apparently is that the gluino has been integrated out at $Q \simeq 600$ GeV, and its effect on the squark soft masses is to *increase* their values during running from $M_{\rm GUT}$ to $m_{\tilde{t}_{L,R}}$.

V. IMPROVED ISAJET: EFFECT ON THE COMPLETE SPECTRUM

In order to improve on the problems discussed above, the new version of Isajet, v7.73, adopts the following scheme:

TABLE IV. SPheno 2.2.3 results (masses in GeV) for the scalar top sector at SPS1a.

Q	$M_{\tilde{Q}_3}$	$M_{\tilde{U}_3}$	A_t	$m_{\tilde{t}_1}^{\overline{\rm DR}}$	$m_{\tilde{t}_2}^{\overline{\rm DR}}$	$\theta_{\tilde{t}}^{\overline{\rm DR}}$	$m_{\tilde{t}_1}^{\rm pole}$	$m_{\tilde{t}_2}^{\rm pole}$	$\theta_{\tilde{t}}^{\rm pole}$
100	533.8	454.6	−524.4	414.1	607.0	56.5°	395.8	577.0	56.4°
200	516.3	438.7	−508.9	398.7	588.5	56.4°	399.6	582.2	56.4°
$M_{\rm SUSY}$	495.5	419.9	−490.4	380.2	566.2	56.3°	400.6	586.0	56.4°
1000	479.6	405.5	−476.3	366.2	549.6	56.2°	399.0	585.2	56.3°

TABLE V. Isajet results (masses in GeV) for the scalar top sector at SPS1a. Case A is the result of Isajet 7.72; Case B is Isajet 7.72 with the improvement that the one-loop self-energies are each computed at their relevant scale; Case C employs step-beta functions for all SUSY parameters. In case D, the SUSY parameters are all frozen out at $Q = \sqrt{m_{\tilde{t}_L} m_{\tilde{t}_R}} \simeq 456$ GeV, and the one-loop corrections are applied at this scale.

Case	$M_{\tilde{Q}_3}$	$M_{\tilde{U}_3}$	A_t	$m_{\tilde{t}_1}^{(0)}$	$m_{\tilde{t}_2}^{(0)}$	$\theta_{\tilde{t}}^{(0)}$	$m_{\tilde{t}_1}^{(1)}$	$m_{\tilde{t}_2}^{(1)}$	$\theta_{\tilde{t}}^{(1)}$
A	493.7	422.5	−496.6	381.2	566.4	55.7°	401.8	583.5	56.8°
B	493.6	422.4	−496.4	381.2	566.4	55.7°	405.7	584.9	57.0°
C	488.5	414.3	−489.7	373.7	560.1	56.0°	394.1	577.2	57.2°
D	495.3	420.6	−498.5	379.8	566.6	56.2°	400.0	583.9	57.2°

TABLE VI. Results of Isajet and SPheno for SPS1a. Isajet 7.73 is the new version, which includes the improvements explained in the text; $\delta^{\rm scale}$ is the scale dependence for $Q = 0.1$–1 TeV in SPheno 2.2.3. All values in GeV.

Mass	Isajet 7.72	Isajet 7.73	SPheno 2.2.3	$\delta^{\rm scale}$
$\tilde{\chi}_1^0$	95.19	97.39	97.11	0.3
$\tilde{\chi}_2^0$	180.5	180.4	180.7	1.1
$\tilde{\chi}_3^0$	356.7	358.7	364.9	0.6
$\tilde{\chi}_4^0$	377.2	379.0	382.2	0.3
$\tilde{\chi}_1^\pm$	180.4	180.3	180.3	1.1
$\tilde{\chi}_2^\pm$	376.2	378.0	383.3	0.4
$\tilde{e}_L$	203.2	203.3	202.4	0.3
$\tilde{e}_R$	144.0	142.5	144.1	0.8
$\tilde{\nu}_e$	187.1	185.5	186.2	0.2
$\tilde{\tau}_1$	134.8	134.6	134.4	0.6
$\tilde{\tau}_2$	206.7	205.9	206.4	0.3
$\tilde{\nu}_\tau$	186.2	183.4	185.3	0.2
$\tilde{u}_L$	559.5	564.9	565.1	9.8
$\tilde{u}_R$	544.0	548.6	547.8	8.9
$\tilde{d}_L$	565.2	570.9	570.5	9.7
$\tilde{d}_R$	543.7	548.2	547.8	8.9
$\tilde{t}_1$	401.8	395.2	400.6	5.0
$\tilde{t}_2$	583.5	584.4	586.0	9.0
$\tilde{b}_1$	516.5	518.6	514.9	7.9
$\tilde{b}_2$	539.7	547.1	547.5	8.7
$\tilde{g}$	611.4	605.9	604.3	1.3

(1) The running parameters of nonmixing sparticles, i.e. squarks and sleptons of the first and second generation, and the gluino, are extracted at their respective mass scale. The one-loop radiative corrections are implemented at this scale, which is also taken to be the renormalization scale. Thus, double counting of logarithmic corrections is not present.

(2) The parameters of mixing sparticles, i.e. neutralinos, charginos, stops, sbottoms, and staus, are all extracted at the scale $Q = \sqrt{m_{\tilde{t}_L} m_{\tilde{t}_R}}$, which is also taken to be the renormalization scale. Diagonalization of the mass matrices are performed once for each sparticle mass, with self-energies evaluated at the corresponding sparticle's tree-level mass.

(3) The implementation of variable beta functions for the SUSY parameters is postponed until a consistent treatment of logarithmic and finite corrections for multiple scales is available.

In addition, in Isajet 7.73, the gluino mass radiative corrections depending on squark mixing have been added; these mixing corrections were absent in previous Isajet versions. The results of Isajet 7.73 are given in Table VI and compared with those of Isajet 7.72 and SPheno 2.2.3. Also shown is the scale dependence in SPheno 2.2.3.

At this point it is important to note that the remaining differences in the spectra of Isajet 7.73 and SPheno 2.2.3 cannot be attributed exclusively to the different methods of implementing SUSY thresholds to the SUSY parameters. There are analogous differences in the implementation of supersymmetric thresholds to the gauge and Yukawa couplings. In both programs, the experimental central values of the SM gauge couplings and third-generation fermion masses are used to determine the low-energy boundary conditions for the gauge and Yukawa couplings in the $\overline{\rm DR}$ scheme. These are then extrapolated up to the GUT scale, defined as the scale where $\alpha_1 = 5\alpha_e/3(1 - s_W^2)$ and $\alpha_2 = \alpha_e/s_W^2$ unify. SPheno, as well as SoftSusy and Suspect, use a one-step implementation of the supersymmetric (log+finite) corrections to gauge and Yukawa couplings with the matching between SM and MSSM couplings done at the scale M_Z. In Isajet, on the other hand, logarithmic thresholds are implemented in a one-by-one decoupling from the RG equations each time a threshold is passed, while finite corrections are implemented collectively at a common scale. The boundary conditions at the GUT scale are therefore not going to be identical. This is exemplified in Table VII, where we show the GUT-scale values of the gauge and Yukawa couplings from Isajet and SPheno at SPS1a. We see that there is no perfect gauge coupling unification since $\alpha_3 \neq \alpha_1 = \alpha_2$. The unification degree is of the order of 1.5%. This is expected for two-loop RGEs and can be attributed to threshold effects due to particles with GUT-scale masses. The differences between Isajet 7.73 and SPheno 2.2.3 amount to 8% for the GUT scale (which enters logarithmically in the RGEs), 1% for the unified gauge coupling, 2% for the top and 8% for the bottom Yukawa couplings. We

TABLE VII. Comparison of $\overline{\rm DR}$ GUT-scale gauge and Yukawa couplings obtained from Isajet 7.72, Isajet 7.73 and SPheno 2.2.3 for the benchmark point SPS1a.

GUT output	Isajet 7.72	Isajet 7.73	SPheno 2.2.3
$M_{\rm GUT}$	2.28×10^{16} GeV	2.28×10^{16} GeV	2.46×10^{16} GeV
$g_1(M_G) = g_2(M_G)$	0.715	0.715	0.721
$g_3(M_G)$	0.706	0.706	0.707
$h_t(M_G)$	0.505	0.516	0.527
$h_b(M_G)$	0.049	0.047	0.051
$h_\tau(M_G)$	0.068	0.068	0.068

conclude that even for a "well behaved" point such as SPS1a the differences in the GUT-scale output cannot be neglected; in studies of Yukawa unified models they can become crucial.

VI. DISCUSSION OF THE MULTISCALE APPROACH

Integrating out all SUSY particles at a common scale is a reliable procedure if their masses are all in roughly the same ballpark. This is, for example, the case for the SPS1a benchmark point. However, in the case where the SUSY spectrum [including the Higgs bosons] is spread over a large range of masses, one should get more precise predictions by integrating out the SUSY particles at various scales. Consider for instance the gluino mass. In the common scale approach

$$m_{\tilde{g}}^{\text{pole,CS}} = M_3(Q) + \Delta m_{\tilde{g}}(Q), \tag{9}$$

while if the gluino is frozen out at its own mass scale,

$$m_{\tilde{g}}^{\text{pole,MS}} = M_3(M_3) + \Delta m_{\tilde{g}}(M_3). \tag{10}$$

At SPS1a with $M_{\tilde{Q}} \sim 550$ GeV and $M_3 \sim 600$ GeV, we find $m_{\tilde{g}}^{\text{pole,CS}} = 604.3$ GeV and $m_{\tilde{g}}^{\text{pole,MS}} = 604.1$ GeV, i.e. excellent agreement between the two methods. If we move, however, M_3 to $M_3(M_3) = 1.8$ TeV, we find $m_{\tilde{g}}^{\text{pole,CS}} = 1512$ GeV, and $m_{\tilde{g}}^{\text{pole,MS}} = 1531$ GeV—i.e. a spread of 19 GeV. A multiscale treatment of thresholds therefore seems desirable when the spectrum is considerably split.

In the following, we outline the implications of a consistent multiscale approach. To work out a complete prescription is, however, beyond the scope of this Letter. Technically, at each scale a new effective theory (EFT) has to be constructed, and one faces the following difficulties:

A. Finite shifts

The naive way to take out particles from the RGEs via step functions (as done e.g. in [15]) and to use continuous matching conditions for the remaining parameters holds only for the lowest-order RGEs. At higher orders, finite shifts have to be introduced, as has been known for a long time [17–21]. The simplest example is gauge coupling unification in $SU(5)$ theories: at lowest order, i.e. using one-loop RGEs, the boundary conditions at M_{GUT} are given by $g_{\text{U(1)}} = g_{\text{SU(2)}} = g_{\text{SU(3)}} = g_{\text{SU(5)}}$. At next-to-leading and higher orders, finite threshold corrections due to particles with masses of order M_{GUT} have to be taken into account [17,20,21], spoiling the lowest-order equality of the gauge couplings. Another prominent example is the evolution of the strong coupling between the scale of the lightest quarks and m_Z: see e.g. [22].

In our case, we are working with two-loop (or higher loop) RGEs for the SUSY parameters, as for the gauge and Yukawa couplings. In this case, when integrating out SUSY particles at various scales, two issues have to be taken into account: (i) The shifts of the $\overline{\text{DR}}$ parameters of the sparticle that is integrated out to its pole-mass parameters involve contributions of all particles, which are degrees of freedom of the current EFT. (ii) The field(s) that are integrated out also lead to finite shifts in the boundary conditions of the parameters which remain in the RGEs. Take as an example the case where the gluino is the heaviest MSSM particle. At $Q = |M_3|$ the gluino can be integrated out and the pole gluino mass $m_{\tilde{g}}$ is obtained by taking into account the shifts from all strongly interacting particles (at the one-loop level; at the two-loop level all particles contribute in principle). In addition, there will be finite shifts for α_s, the Yukawa couplings (or equivalently the masses) of the quarks, and the squark parameters. A similar effect has been known in QCD for a long time, where the decoupling of heavy quarks also leads to shifts for the boundary conditions of running masses of the lighter quarks [23].

B. New couplings

By integrating out part of the spectrum it may happen that the symmetry of the EFT is "smaller" than the symmetry of the underlying theory. In this case, there arise additional parameters in the EFT. Moreover, there are in general higher-dimensional operators compatible with the reduced symmetry; well known examples of this are the neutrino mass operator in the see-saw mechanism [24] or the operators governing rare meson/baryon decays.

In the case of supersymmetric theories, there is a well studied and important example, namely, the Higgs sector. Within the MSSM, supersymmetry requires that three of the seven couplings of a general 2-Higgs doublet model be zero and that the remaining four be expressed by gauge couplings (at least at tree level). Integrating out the SUSY particles does not only lead to finite shifts for the four nonzero couplings, but also introduces nonzero values for the couplings which are zero due to supersymmetry [25]. In the very same sector, a further complication arises if the top quark is integrated out, as SU(2) is broken in such a case. This leads to various new couplings to the W and Z bosons, each governed by its own RGE [25].

A second important example in this context is the bottom Yukawa coupling. If one integrates out, e.g. the gluino, from the spectrum, one induces nonholomorphic Yukawa couplings between the quark fields and the Higgs fields, e.g. a $b\bar{b}H_u$ coupling [26].

The complete set of superfield operators leading to dimension 5 and 6 operators in the Lagrangian has been worked out for the MSSM [27], assuming that it is the effective theory of a more fundamental one. If one regards the MSSM as fundamental and integrates out part of it, the

operators obtained will form a subset of those given in [27]. The techniques to obtain the tree-level coefficients in front of these operators have been elaborated in [28].

C. Sparticle mixing

Clearly, once from a set of mixing particles the heavier ones are integrated out, the question arises of how to obtain the mixing effects that are visible in the case of a one-step decoupling. The answer is that the above mentioned higher-dimensional operators introduce these effects. Let us sketch this for the stops, for the case when $m^2_{\tilde{t}_L} \gg m^2_{\tilde{t}_R}$. Integrating out $\tilde{t}_L$ yields, for example, effective operators of the form

$$c_1 \frac{g A_t Y_t}{m^2_{\tilde{t}_L}} \tilde{t} P_R \tilde{W}_3 H^0_u \tilde{t}_R, \qquad c_2 \frac{-g \mu Y_t}{m^2_{\tilde{t}_L}} \tilde{t} P_R \tilde{W}_3 H^0_d \tilde{t}_R \quad (11)$$

$$\begin{aligned} c_3 \frac{|A_t Y_t|^2}{m^2_{\tilde{t}_L}} H^0_u H^{0*}_u \tilde{t}_R \tilde{t}^*_R, \qquad c_4 \frac{|\mu Y_t|^2}{m^2_{\tilde{t}_L}} H^0_d H^{0*}_d \tilde{t}_R \tilde{t}^*_R, \\ c_5 \frac{-A_t \mu Y_t^2}{m^2_{\tilde{t}_L}} H^0_d H^{0*}_u \tilde{t}_R \tilde{t}^*_R + \text{h.c.}. \end{aligned} \quad (12)$$

After electroweak symmetry breaking, the operators of the first line contribute to the $\tilde{t}_1 t \tilde{\chi}^0_i$ vertices, whereas those of the second line give contributions to the mass of the lighter stop. The coefficients c_i contain the information of the evolution of the operators from the scale $m_{\tilde{t}_L}$ down to $m_{\tilde{t}_1}$. As a check that these operators really mimic the effect of mixing, let us calculate the stop mixing angle for this case, taking into account that the left stop mass is much larger than the $m_{\tilde{t}_1}$ and m_t (and thus the off-diagonal element):

$$\begin{aligned} \cos\theta_{\tilde{t}} &= \frac{-m_t(A_t - \mu \cot\beta)}{\sqrt{(m^2_{\tilde{t}_L} - m^2_{\tilde{t}_1})^2 + m_t^2 (A_t - \mu \cot\beta)^2}} \\ &\simeq \frac{-m_t(A_t - \mu \cot\beta)}{m^2_{\tilde{t}_L}}. \end{aligned} \quad (13)$$

At the scale $m_{\tilde{t}_L}$, $c_i = 1 \,\forall\, i$, and thus if one naively replaces the Higgs fields by $v_{u,d}/\sqrt{2}$ and $\tilde{t}_R$ by $\tilde{t}_1$ one obtains exactly the coupling of the lighter stop to the neutral wino in Eq. (11) and the contribution of the left stop to the lighter stop mass in Eq. (12). We note that the case of $c_i = 1$ is also obtained if one applies the see-saw formula to the stop sector.

VII. CONCLUSIONS

We have discussed the two general methods of treating threshold effects in the computation of sparticle pole masses from high-scale input: (a) renormalization at a common SUSY scale and (b) freezing out each sparticle at its own mass scale. We have focused, in particular, on the concrete implementations of these methods in SPheno 2.2.3 and Isajet 7.72 and compared the results of these programs for the SPS1a benchmark point. Several shortcomings were pointed out, together with suggestions for improvements. The new version Isajet 7.73 incorporates these improvements, leading to better agreement between the various codes, especially for the LSP mass but also for the squark and gluino masses.

Integrating out all SUSY particles at a common scale, as done in SoftSusy, SPheno and Suspect, is a reliable procedure if their masses are all in roughly the same ballpark. The results of the alternative method followed in Isajet are in good agreement with this procedure. (Here, note that the method applied in Isajet is not a complete multiscale but a hybrid approach.) In order to match the ultrahigh accuracy expected at the ILC, a consistent multiscale treatment of SUSY threshold effects seems necessary. The method is in principle well known from QCD. At each scale where a threshold is passed, the relevant field(s) have to be taken out of the RGEs and a new effective theory has to be constructed below the threshold. The shifts of the $\overline{\text{DR}}$ to the pole-mass parameters of the sparticle that is integrated out involve contributions of all the particles that are degrees of freedom of the current EFT. Moreover, the field(s) that are integrated out lead to finite shifts in the boundary conditions of the parameters which remain in the EFT, so we face nontrivial matching conditions. Additional complications arise when the symmetry of the EFT is ''smaller'' than the symmetry of the underlying theory. We have outlined this multiscale approach in Sec. VI and discussed its technical implications. A complete prescription for the matching over multiple scales is, however, beyond the scope of this Letter and will be explored in the future.

ACKNOWLEDGMENTS

The work of S. K. is financed by an APART (Austrian Programme of Advanced Research and Technology) grant of the Austrian Academy of Sciences. W. P. is supported by a MCyT Ramon y Cajal contract, by the Spanish grant BFM2002-00345, by the European Commission, Human Potential Program RTN network HPRN-CT-2000-00148, and partly by the Swiss ''Nationalfonds''.

[1] G. A. Blair, W. Porod, and P. M. Zerwas, Phys. Rev. D **63**, 017703 (2001); Eur. Phys. J. C **27**, 263 (2003).
[2] B. C. Allanach *et al.*, Nucl. Phys. B, Proc. Suppl. **135**, 107 (2004); Nucl. Phys. B, Proc. Suppl. **135**, 107 (2004).
[3] G. Weiglein *et al.* (LHC/LC Study Group), hep-ph/0410364.
[4] Supersymmetry Parameter Analysis (SPA) project, http://spa.desy.de/spa/
[5] B. C. Allanach, S. Kraml, and W. Porod, J. High Energy Phys. 03 (2003) 016.
[6] F. E. Paige, S. D. Protopescu, H. Baer, and X. Tata, hep-ph/0312045.
[7] B. C. Allanach, Comput. Phys. Commun. **143**, 305 (2002).
[8] W. Porod, Comput. Phys. Commun. **153**, 275 (2003).
[9] A. Djouadi, J. L. Kneur, and G. Moultaka, hep-ph/0211331.
[10] Online comparison of SUSY spectrum computations, http://cern.ch/kraml/comparison
[11] B. C. Allanach, G. Bélanger, F. Boudjema, and A. Pukhov, J. High Energy Phys. 12 (2004) 020; B. C. Allanach, G. Bélanger, F. Boudjema, A. Pukhov, and W. Porod, hep-ph/0402161; G. Bélanger, S. Kraml, and A. Pukhov, Phys. Rev. D **72**, 015003 (2005).
[12] D. M. Pierce, J. A. Bagger, K. T. Matchev, and R. j. Zhang, Nucl. Phys. **B491**, 3 (1997).
[13] G. Degrassi, P. Slavich, and F. Zwirner, Nucl. Phys. **B611**, 403 (2001); A. Brignole, G. Degrassi, P. Slavich, and F. Zwirner, Nucl. Phys. **B631**, 195 (2002); Nucl. Phys. **B643**, 79 (2002); A. Dedes and P. Slavich, Nucl. Phys. **B657**, 333 (2003); B. C. Allanach *et al.*, J. High Energy Phys. 09 (2004) 044.
[14] D. J. Castano, E. J. Piard, and P. Ramond, Phys. Rev. D **49**, 4882 (1994.
[15] A. Dedes, A. B. Lahanas, and K. Tamvakis, Phys. Rev. D **53**, 3793 (1996).
[16] W. Oller, H. Eberl, W. Majerotto, and C. Weber, Eur. Phys. J. C **29**, 563 (2003).
[17] S. Weinberg, Phys. Lett. B **91**, 51 (1980).
[18] B. A. Ovrut and H. J. Schnitzer, Phys. Lett. B **100**, 403 (1981).
[19] B. A. Ovrut and H. J. Schnitzer, Nucl. Phys. **B179**, 381 (1981).
[20] L. J. Hall, Nucl. Phys. **B178**, 75 (1981).
[21] P. Binétruy and T. Schucker, Nucl. Phys. **B178**, 307 (1981).
[22] K. G. Chetyrkin, B. A. Kniehl, and M. Steinhauser, Nucl. Phys. **B510**, 61 (1998).
[23] W. Wetzel, Nucl. Phys. **B196**, 259 (1982).
[24] P. Minkowski, Phys. Lett. B **67**, 421 (1977); M. Gell-Mann, P. Ramond, and R. Slansky, in *Proc. of the Workshop on Complex Spinors and Unified Theories, Stony Brook, New York* (North-Holland, Amsterdam, 1979); T. Yanagida KEK Report No. 79-18, 1979 (unpublished); R. N. Mohapatra and G. Senjanovic, Phys. Rev. Lett. **44**, 912 (1980).
[25] H. E. Haber and R. Hempfling, Phys. Rev. D **48**, 4280 (1993).
[26] M. Carena, D. Garcia, U. Nierste, and C. E. M. Wagner, Nucl. Phys. **B577**, 88 (2000); A. Dedes and A. Pilaftsis, Phys. Rev. D **67**, 015012 (2003); H. Eberl, K. Hidaka, S. Kraml, W. Majerotto, and Y. Yamada, Phys. Rev. D **62**, 055006 (2000).
[27] D. Piriz and J. Wudka, Phys. Rev. D **56**, 4170 (1997).
[28] E. Katehou and G. G. Ross, Nucl. Phys. **B299**, 484 (1988); J. Leén, J. Pérez-Mercader, and M. F. Sánchez, Phys. Lett. B **208**, 463 (1988); Phys. Lett. B **221**, 324 (1989).